

Imaging the External Ear: Practical Approach to Normal and Pathologic Conditions

Niedja S. G. Tsuno, MD

Marco Y. Tsuno, MD

Carlos A. F. Coelho Neto, MD

Samir E. Noujaim, MD

Marcos Decnop, MD

Felipe T. Pacheco, MD, PhD

Soraia A. Souza, MD, PhD

Ana P.A. Fonseca, MD

Marcio R. T. Garcia, MD

Abbreviations: EAC = external auditory canal; EE = external ear; KO = keratosis obturans; TMJ = temporomandibular joint

RadioGraphics 2022; 42:522–540

<https://doi.org/10.1148/rg.210148>

Content Codes: **CT** **HN** **MR** **NR**

From the Divisions of Neuroradiology (N.S.G.T.) and Musculoskeletal Radiology (M.Y.T.), Laboratório Exame, Diagnósticos da América SA, SHLN, Lote 09, Bloco G, Asa Norte, Brasília, DF, Brazil 70770560; Divisions of Head and Neck Imaging (C.A.F.C.N., S.A.S., M.R.T.G.) and Neuroradiology (F.T.P., A.P.A.F.), Laboratórios Alta Excelência Diagnóstica e Delboni Auríromo, Diagnósticos da América SA, São Paulo, Brazil; Department of Head and Neck Radiology, Oakland University School of Medicine, Beaumont Health System, Royal Oak, Mich (S.E.N.); and Division of Head and Neck Imaging, Instituto Nacional do Câncer (INCA), Rio de Janeiro, Brazil (M.D.). Presented as an education exhibit at the 2020 RSNA Annual Meeting. Received April 26, 2021; revision requested June 16 and received July 14; accepted July 20. For this journal-based SA-CME activity, the authors, editor, and reviewers have disclosed no relevant relationships. **Address correspondence to** N.S.G.T. (e-mail: niedjatsuno@gmail.com).

©RSNA, 2022

SA-CME LEARNING OBJECTIVES

After completing this journal-based SA-CME activity, participants will be able to:

- Discuss the fundamental anatomy and developmental concepts of the EE.
- Distinguish the imaging features of normal anatomic variations of the EE from those of pathologic conditions.
- Recognize the main diseases of the EE.

See www.rsna.org/education/search/RG.

The external ear (EE) is an osseous-cartilaginous structure that extends from the auricle to the tympanic membrane. It is divided into two parts: the auricle (or pinna) and the external auditory canal (EAC). Given the ease of access to the EE, imaging studies are not always needed to make a diagnosis. However, when lesions block visual access to areas deep to the EE abnormality, complications are suspected, or there is lack of response to treatment, imaging becomes essential. A basic understanding of the embryologic development and knowledge of the anatomy of the auricle and EAC are useful for accurate diagnosis of EE lesions. Congenital, traumatic, inflammatory, neoplastic, and vascular conditions can affect the EE. An overview of the anatomy and embryologic development of the EE is presented, with discussion and illustrations of common and uncommon conditions that affect EE structures and a focus on the CT and MRI features that are of interest to radiologists. CT is usually the first diagnostic modality used to evaluate the EAC and is the superior method for demonstrating bone changes. MRI provides excellent tissue characterization and enables one to better define lesion extension and perineural tumor spread. In addition, a flowchart to facilitate the differential diagnosis of EE abnormalities is provided.

Online supplemental material is available for this article.

©RSNA, 2022 • radiographics.rsna.org

Introduction

The external ear (EE) is anatomically and functionally divided into the cartilaginous auricle, or pinna, and the external auditory canal (EAC). The auricle captures, concentrates, and amplifies sound waves, directing them into the EAC. In turn, the function of the EAC is to conduct sound waves, in the form of vibrations, to the tympanic membrane (1).

The EE can be affected by a variety of conditions, including congenital abnormalities, trauma, inflammatory conditions (infectious or otherwise), vascular anomalies, and neoplasms (benign or malignant) (2). Many of these lesions can be diagnosed clinically; however, diverse pathologic conditions in this region can share similar clinical features. Therefore, imaging may be required to evaluate the extent of a lesion, to evaluate the feasibility of resection, to determine the differential diagnosis, to evaluate for potential complications, and for surgical planning (1).

CT and MRI are the key diagnostic modalities used for evaluation of EE lesions. CT, which is typically the first imaging method used to evaluate the EE, is performed with thin sections and multiplanar reformations, which enable excellent visualization of the bone structures. In contrast, MRI is more specific than CT for differentiating between tumor tissue and inflammatory lesions and enables one to better define the full extension of malignant neoplasms, including perineural

TEACHING POINTS

- The EE can be affected by a variety of conditions, including congenital abnormalities, trauma, inflammatory conditions (infectious or otherwise), vascular anomalies, and neoplasms (benign or malignant).
- Many of these lesions can be diagnosed clinically; however, diverse pathologic conditions in this region can share similar clinical features. Therefore, imaging may be required to evaluate the extent of a lesion, to evaluate the feasibility of resection, to determine the differential diagnosis, to evaluate for potential complications, and for surgical planning.
- The fissures of Santorini are natural openings in the anteroinferior aspect of the cartilaginous portion of the EAC. Although these fissures are not visible at imaging owing to their small size, they serve as a potential pathway for the spread of infection and neoplastic processes in both directions, from the parotid space and TMJ into the EAC, or vice versa.
- CT is ideal for evaluation of bone erosions, especially those in the floor of the EAC and skull base, and is useful for detecting soft-tissue abnormalities outside of the temporal bone. MRI provides the most anatomically detailed information about disease extension into soft tissues and bone marrow.
- MRI also enables better evaluation of tumor extension to the TMJ and parotid gland, as well as to the soft tissues around the ear, by depicting replacement of the T1-hyperintense fatty tissues with intermediate T1 signal intensity tumor, which also shows diffusion restriction and contrast enhancement.

spread (3,4). In many cases, CT and MRI have complementary roles in the diagnostic evaluation.

The most widely used CT protocol for EE examination involves multisector volumetric acquisition with high-spatial-resolution submillimeter-thin sections (thickness between 0.5 mm and 1.0 mm), followed by multiplanar reconstructions with soft- and bone-tissue algorithms. The typical MRI examination involves use of a small field of view (15–18 cm) and a thin section thickness (2 mm). This protocol includes acquisition of axial and coronal T1- and T2-weighted MR images, use of a heavily T2-weighted volumetric sequence, and axial diffusion-weighted imaging. Axial and coronal T1-weighted fat-suppressed MR images are acquired after intravenous injection of gadolinium-based contrast material (3,4).

Anatomy

The temporal bone is composed of five parts: squamous, mastoid, petrous, tympanic, and styloid portions (5). The tympanic part of the temporal bone forms the EAC proper. It is inferior to the squamous part of the bone and anterior to the mastoid portion. The tympanosquamous fissure (Fig E1) separates the tympanic part of the temporal bone from the squamous portion. It is parallel and anterior to the bony EAC. The tympanomastoid fissure (Fig E1), which is not always open, is located posteriorly, parallel to the

bony EAC, separating the tympanic part of the EAC from the mastoid portion.

The EE includes the auricle and the EAC. The EE is separated from the middle ear by the tympanic membrane. The main anatomic structures of the EE are summarized in Figure 1. The auricle consists of elastic cartilage that is covered on both anterior and posterior surfaces with thin hairy skin. The ear lobe, located in the lower pole of the auricle, is covered with skin and contains fibrous tissue, fat, and small blood vessels, but no cartilage (2).

The EAC is divided into two parts: the lateral one-third and the medial two-thirds of the canal. The lateral third of the EAC is the fibrocartilaginous portion; it is continuous with the auricle, lined with skin, and contains hair follicles, sebaceous glands, and ceruminous glands, which produce a waxy exudate called cerumen. The medial two-thirds of the EAC make up the bony canal, which is limited medially by a shallow bone ridge, the tympanic annulus, to which the tympanic membrane is attached. The bony canal is lined with very thin skin, closely adherent to the underlying periosteum, and is continuous with the external layer of the tympanic membrane. The narrowest part of the EAC is the isthmus, which separates the cartilaginous part from the bony segment. The cartilaginous portion of the EAC is oriented in a posterosuperior direction, while the bony portion is oriented in an anteroinferior direction (2).

The anterior wall of the EAC also constitutes the posterior wall of the temporomandibular joint (TMJ). The posterior wall of the EAC forms the anterior margin of the mastoid segment of the temporal bone (5). The EAC in adults measures approximately 2.5 cm in length. In infants, the EAC is almost entirely cartilaginous.

The fissures of Santorini are natural openings in the anteroinferior aspect of the cartilaginous portion of the EAC (Fig 1). Although these fissures are not visible at imaging owing to their small size, they serve as a potential pathway for the spread of infection and neoplastic processes in both directions, from the parotid space and TMJ into the EAC, or vice versa (Fig 2) (5,6).

A persistent foramen tympanicum, or foramen of Huschke, is an anatomic variation of the tympanic portion of the temporal bone that is due to a defect in normal ossification during the first 5 years of life. This foramen is located at the anteroinferior aspect of the EAC, posteromedial to the TMJ. Foramen tympanicum is considered a permanent defect only after the individual is aged 5 years (Fig 3).

A foramen tympanicum may permit spontaneous herniation of soft tissue from the TMJ into the EAC, which can cause TMJ pain and dysfunction.

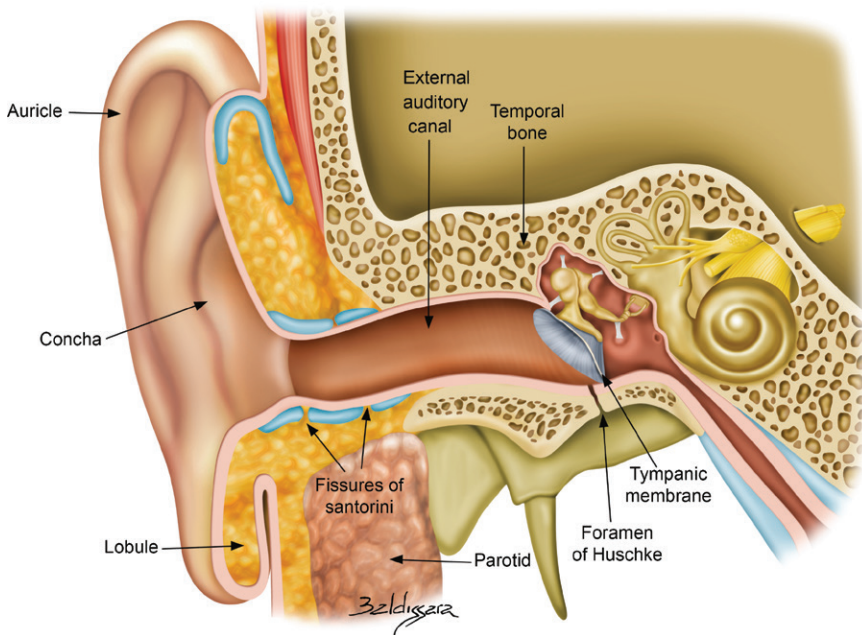


Figure 1. Drawing depicts the main anatomic structures of the EE.

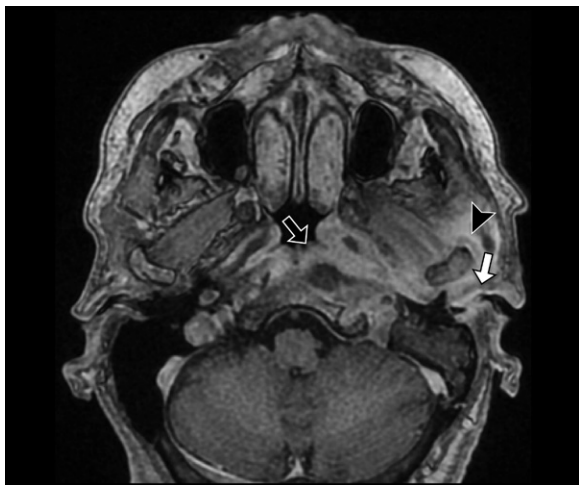


Figure 2. Septic arthritis of the TMJ, with extension to the EAC through the anterior wall and Santorini fissure. Axial contrast-enhanced T1-weighted MR image shows an aggressive inflammatory process originating from the TMJ (arrowhead) and extending to the nasopharynx (black arrow) and EAC (white arrow).

Synovial fluid can extravasate into the EAC and cause ear discharge, especially during mastication. The parotid gland can extend to the glenoid fossa behind the TMJ and lie near the osseous portion of the EAC; salivary fluid can also extravasate into the EAC. The soft tissue within the EAC usually disappears with opening of the mouth. Conversely, lesions affecting the EAC can extend through this defect into the TMJ (6).

Embryologic Development

A detailed description of the embryologic development of the temporal bone is beyond the



Figure 3. Foramen of Huschke, or foramen tympanicum. Axial bone-window CT image shows the foramen of Huschke (arrows) in a healthy patient, characterized by a developmental defect in the anteroinferior aspect of the bony portion of the EAC, posteromedial to the TMJ.

scope of this article. The branchial apparatus structures develop between the 4th and 6th weeks of gestation and consist of the six pairs of mesodermal branchial arches separated by five paired ectodermal branchial clefts (grooves) externally and five paired endodermal pharyngeal pouches internally. The ear is derived primarily from the first branchial apparatus, with contributions from the second branchial apparatus.

The first branchial cleft gives rise to the EAC (7). The first arch gives rise to the mandible, muscles of mastication, malleus, incus, auricle, and mandibular division of cranial nerve V, while the eustachian tube, tympanic cavity, and mastoid air cells derive from the first pouch. The second cleft involutes, and the second arch gives

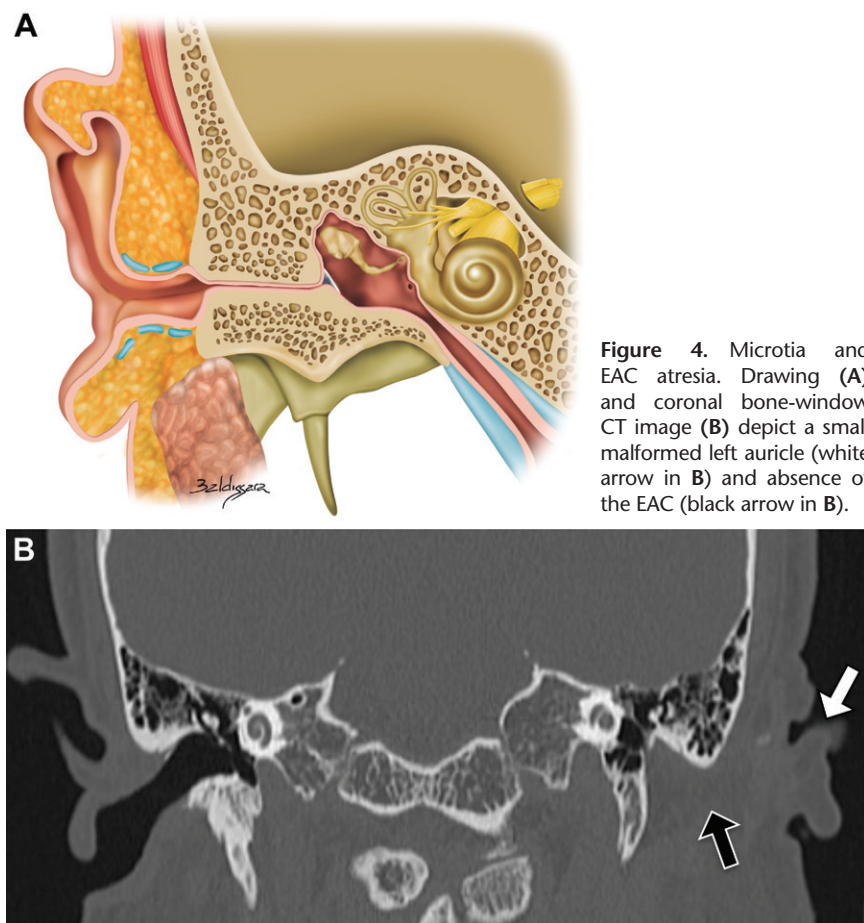


Figure 4. Microtia and EAC atresia. Drawing (A) and coronal bone-window CT image (B) depict a small malformed left auricle (white arrow in B) and absence of the EAC (black arrow in B).

rise to the muscles of facial expression, body and lesser horn of the hyoid bone, stapes, and cranial nerves VII and VIII. The palatine tonsils originate from the second pouch (8).

In 1885, Wilhelm His described six auricular hillocks that give shape to the human auricle: three hillocks on the first pharyngeal arch and three on the second pharyngeal arch. The hillocks of the first pharyngeal arch form the tragus and the helix as far as the auricular tubercle. The hillocks of the second pharyngeal arch form the rest of the auricle, including the lobule. The inner ear (cochlea, vestibule, semicircular canals, internal auditory canal, and vestibular aqueduct) does not grow after birth. Usually, the pinna grows with the rest of the body until an individual is up to 7–10 years of age (7).

Congenital Malformations

Malformations of the EE are referred to as congenital aural dysplasias. They occur in one in 3300 to one in 10 000 births and are most commonly isolated and unilateral, with the right side being more frequently affected (9). However, bilateral malformation is possible and may result from genetic disorders, chromosomal aberrations, and exposure to environmental teratogens.

Auricular Malformations

Most auricular malformations are microtia (underdevelopment), which can affect the size, shape, position, and orientation of the pinna. Complete absence of the pinna, known as anotia, also can occur.

EAC Malformations

Stenosis or incomplete atresia should be suspected when the pinna is abnormal and the EAC diameter is less than 4 mm, or when the tympanic membrane cannot be visualized (Fig 4) (10,11). The stenosis can be fibrous, bony, or both. With the fibrous type, there is a soft-tissue plug at the level of the tympanic membrane, whereas bony stenosis is characterized by a bony plate at the same level (Fig 5). EAC atresia may be part of a congenital malformation syndrome or sequence such as Goldenhar syndrome, Treacher Collins syndrome, or Pierre Robin sequence.

Various classification schemes for grading the severity of the EAC deformity have been proposed. The Weerda classification, which includes three grades of microtia with worsening severity, is widely used for clinical assessment of EAC and auricular malformations (9).

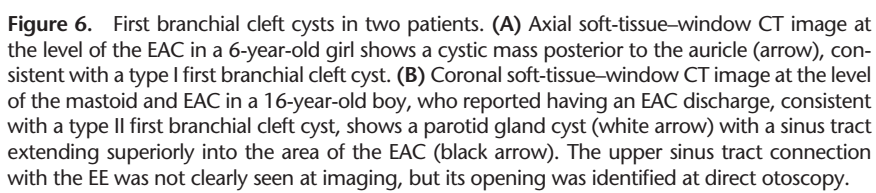
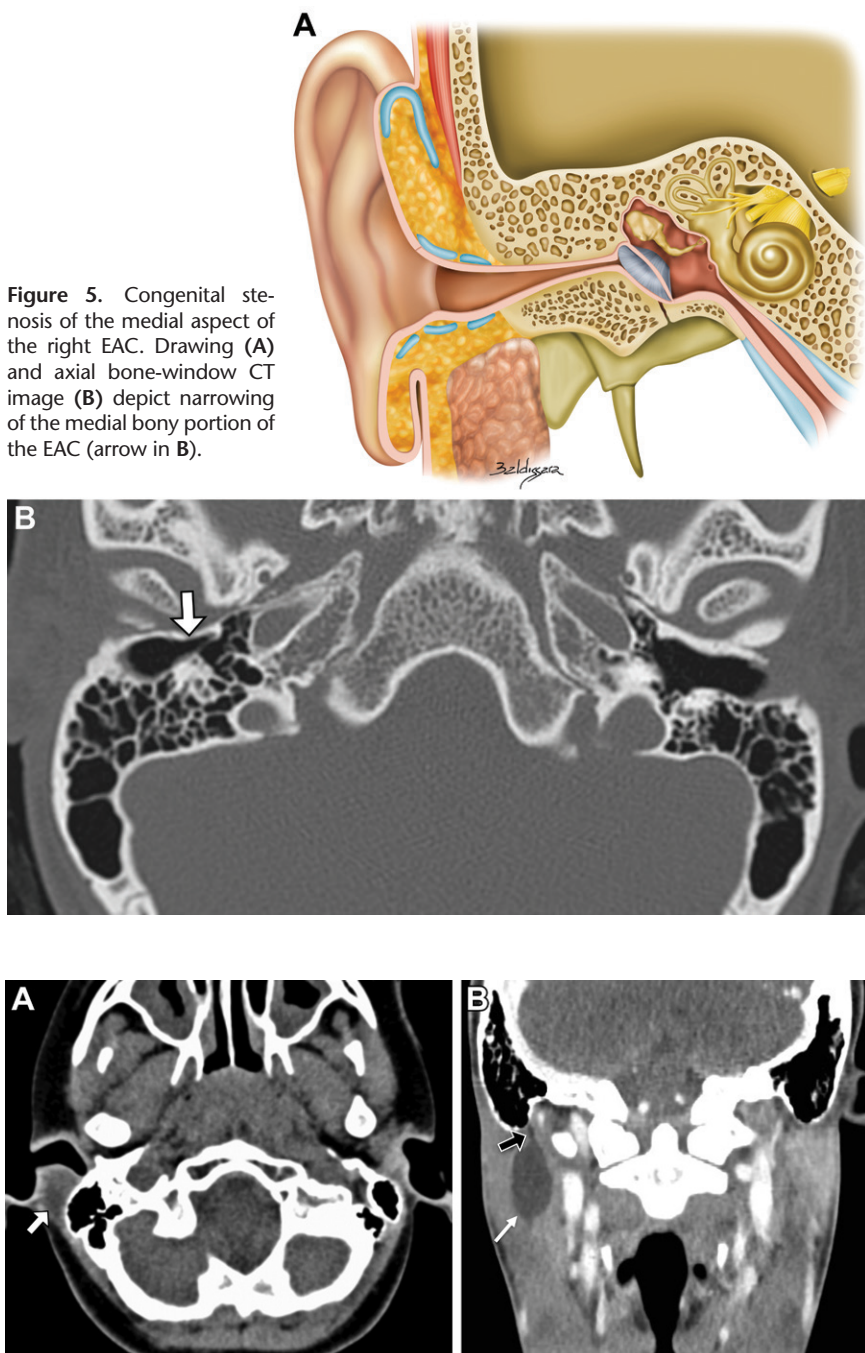


Figure 6. First branchial cleft cysts in two patients. (A) Axial soft-tissue–window CT image at the level of the EAC in a 6-year-old girl shows a cystic mass posterior to the auricle (arrow), consistent with a type I first branchial cleft cyst. (B) Coronal soft-tissue–window CT image at the level of the mastoid and EAC in a 16-year-old boy, who reported having an EAC discharge, consistent with a type II first branchial cleft cyst, shows a parotid gland cyst (white arrow) with a sinus tract extending superiorly into the area of the EAC (black arrow). The upper sinus tract connection with the EE was not clearly seen at imaging, but its opening was identified at direct otoscopy.

First Branchial Cleft Anomalies

First branchial cleft anomalies account for up to 8% of all branchial anomalies and are usually cysts or sinuses near the EAC and/or parotid gland. They result from abnormal ectodermal closure of the first cleft, typically around the periauricular region, anterior or posterior to the pinna, and can extend inferiorly to the angle of

the mandible, either superficially or embedded within the parotid gland (11). The most widely accepted classification of first branchial apparatus cysts was proposed by Work in 1972.

A type I cyst is rare and purely ectodermal and appears histologically as a cystic mass lined by squamous epithelium or a fistula posterior to the pinna (Fig 6A). A type II cyst contains ectoder-

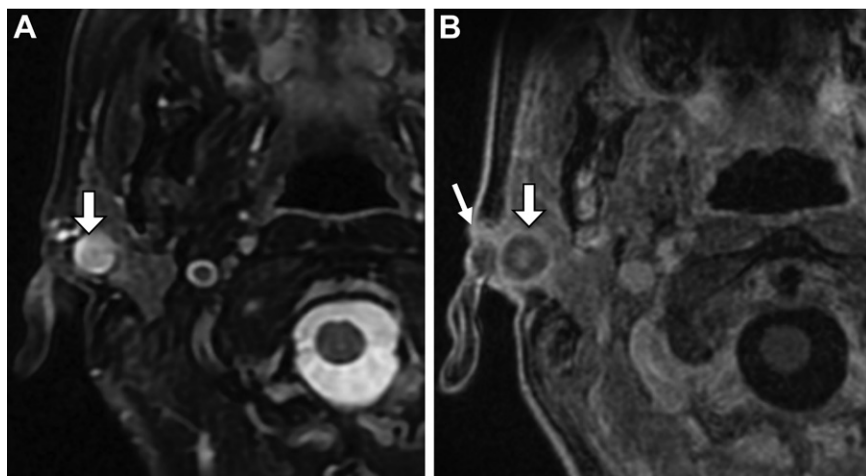


Figure 7. Coloboma auris. Axial T2-weighted fat-suppressed (A) and contrast-enhanced T1-weighted fat-suppressed (B) MR images show a cystic lesion (thick arrow) close to the anterior crus of the right helix, adjacent to the parotid gland. A sinus tract communicates the lesion with the skin surface, with a small opening in the preauricular region (thin arrow in B). The regional edema in A and wall enhancement in B are due to superimposed infection.

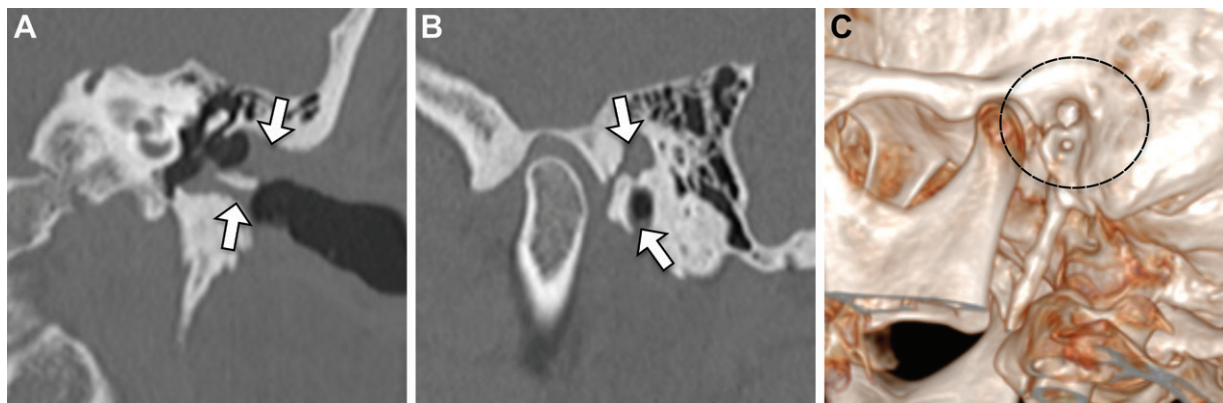


Figure 8. Duplicated EAC. (A, B) Coronal (A) and sagittal (B) bone-window CT images show duplication of the EAC (arrows), separated by a bony septum. (C) Three-dimensional reconstruction image shows the two separate canals (inside the circle).

mal and mesodermal elements and is comparatively more common. It is believed to represent duplication of membranous and cartilaginous portions of the EAC. It contains skin, as well as adnexal structures and cartilage. A type II cyst is often associated with fistulas in the auricle or EAC or with a fistulous opening in the neck (Fig 6b). Type II cysts incorporate portions of the first and second arches, and the cleft (8).

Coloboma auris, also known as preauricular (or more rarely periauricular) sinus or preauricular pit, is a relatively common congenital abnormality. It consists of a blind-ended opening in the EE that is often located at or near the anterior crus of the helix. The diagnosis is made clinically. Most of these sinuses remain asymptomatic, but recurrent infection may cause chronic discharge, repeated abscess formation, and/or scarring (Fig 7) (12).

Duplicated EAC is defined as a second rudimentary EAC coexisting with a normal

EAC (Fig 8). It represents an anomaly of the first branchial cleft and is rare, accounting for 1%–8% of all branchial anomalies (13,14). Duplicated EAC may be seen as a mass bulging from the EAC or a fistula tract opening at the osseous-cartilaginous junction. The middle ear cavity is usually free (13).

Fractures

Fractures of the EAC, including transverse, longitudinal, and mixed-type fractures (Fig 9), may be a direct result of a fracture line extending from any part of the temporal bone (15,16). An EAC fracture may also result from impaction of the mandibular condyle into the posterior wall of the TMJ (15), as seen with high-impact trauma to the jaw, which is usually caused by motor vehicle accidents and falls (17). The tympanic plate is localized between the EAC and glenoid fossa and forms the anterior wall, floor, and part of the posterior wall of the auditory

canal. Tympanic plate fractures often result in EAC stenosis and trismus, especially when the glenoid fossa is involved (16).

Clinically, temporal bone fractures manifest with retroauricular ecchymosis, hemotympanum, otorrhagia (16), TMJ dysfunction, and facial nerve palsy (18). Untreated fractures may lead to canal stenosis, which can be avoided by temporarily packing the canal. This resultant condition highlights the importance of early recognition of these fractures (15). If a cutaneous component is trapped by the fracture, acquired cholesteatoma may occur (16).

EAC fractures are better detected with CT and are more conspicuous when evaluated on oblique reconstructions (Pöschl view) (18). The tympanosquamous and tympanomastoid fissures should not be mistaken for fractures (Fig 9). A persistent foramen tympanicum, which may mimic EAC fracture, represents another potential setting for misdiagnosis. The resilient cartilage of the EE may provide some protection from traumatizing forces, but the EE, especially the auricle, is still exposed to lacerating and avulsing wounds.

Inflammatory and Infectious Diseases

Otitis Externa

Otitis externa is diffuse inflammation of the EAC that may also affect the pinna laterally and the tympanic membrane medially. Patients can present with severe otalgia, jaw pain, itching, tenderness of the tragus and pinna, diffuse ear canal edema and/or erythema, and fullness, with or without hearing loss (19).

A variety of gram-positive and gram-negative bacterial species can be identified in patients with acute otitis externa. However, *Pseudomonas aeruginosa* and *Staphylococcus aureus* are the most common agents encountered (20).

Imaging usually is not required and should be reserved for patients who are immunocompromised. CT images may show thickening of the tympanic membrane and the skin of the EAC. When associated with intraluminal soft tissue filling the bony segment of the EAC, it may lead to the diagnosis of medial canal fibrosis induced by the inflammatory process.

Necrotizing Otitis Externa

Necrotizing (or malignant) otitis externa is an invasive infection of the EAC that typically occurs in older adults with diabetes mellitus and other immunosuppressed patients. *P aeruginosa* is nearly always the etiologic agent. More rarely, necrotizing otitis externa can be caused by fungal organisms such as *Aspergillus* or *Candida*

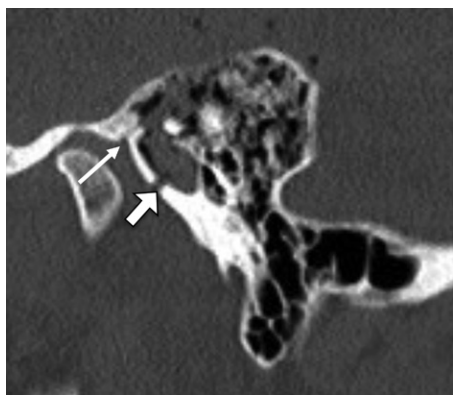


Figure 9. Multiple trauma-related fractures, including EAC fracture. Sagittal bone-window CT image shows a fracture (thick arrow) affecting the anterior wall of the tympanic part of the temporal bone, which should not be confused with the normal tympanosquamous suture seen superiorly (thin arrow). Fluid is seen within the tympanic cavity and mastoid air cells owing to hemotympanum.

species. The diagnosis is based on a combination of clinical and laboratory findings, as well as radiologic evidence of soft-tissue involvement with or without bone erosion in the EAC (21). Spread of infection to adjacent structures usually occurs through the fissures of Santorini or a persistent foramen tympanicum (6).

Imaging is needed to evaluate the extent of involvement and monitor disease progression or remission. The combination of bone and soft-tissue involvement is the most helpful imaging finding for supporting a diagnosis of necrotizing otitis externa (Fig 10) (22). An important complication that can develop in these cases is skull base osteomyelitis, a life-threatening disease caused by extension of infection to the temporal, sphenoid, or occipital bone (23).

CT is ideal for evaluation of bone erosions, especially those in the floor of the EAC and skull base, and is useful for detecting soft-tissue abnormalities outside of the temporal bone (Fig 10). MRI provides the most anatomically detailed information about disease extension into soft tissues and bone marrow. Fat-suppressed and contrast-enhanced MRI sequences can help differentiate phlegmon (enhancement of soft tissues) from soft-tissue abscess (ring enhancement and central necrotic area) (23). In addition, these MR images show the involvement of the retrocondylar fat pad, which can spread via various pathways to extracranial or intracranial spaces (24). This involvement is usually an early finding of necrotizing otitis externa.

MRI is the method of choice for detection of intracranial and cranial nerve involvement. When this occurs, the temporal lobe and cranial

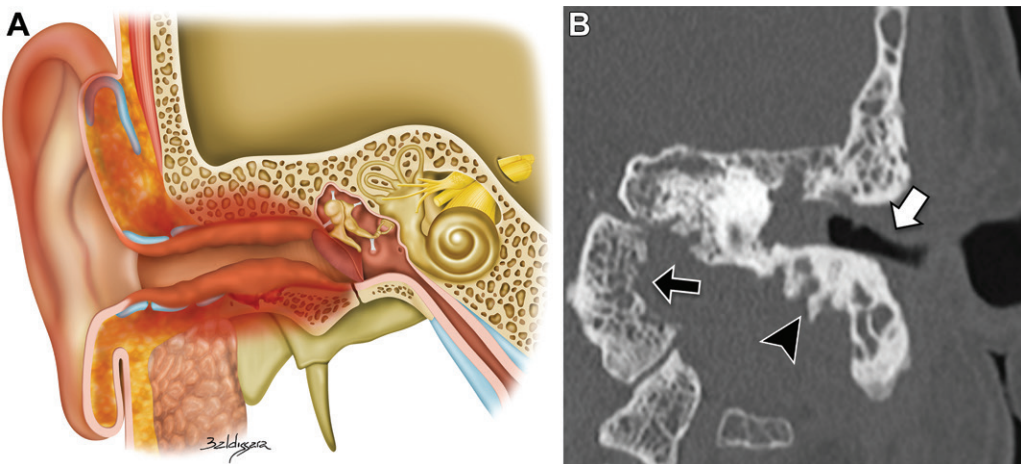


Figure 10. Necrotizing otitis externa. Drawing (A) and coronal bone-window CT image (B) depict skin thickening in the EAC (white arrow in B). Note the extension of the inflammatory process to the skull base on the left, leading to erosion of the jugular tubercle and occipital condyle medially (black arrow in B) and the mastoid bone laterally (arrowhead in B).

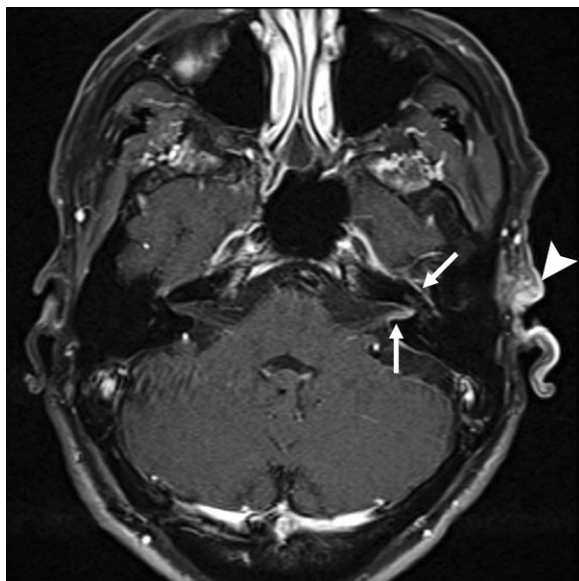


Figure 11. Herpes zoster oticus (ie, Ramsay Hunt syndrome) in a patient with left peripheral nerve palsy, otalgia, and vesicular blisters within the EAC and auricle. Contrast-enhanced T1-weighted fat-suppressed MR image shows abnormal enhancement of the auricle (arrowhead) and the canicular and tympanic segments of the facial nerve (arrows).

nerve VII are the most commonly affected because of their anatomic proximity to the EAC (25). However, the infection may also spread medially to the jugular foramen to involve cranial nerves IX, X, and XI, typically in this order. Jugular vein thrombosis also may occur, owing to inflammation at this site (21).

Nuclear imaging can help confirm bone involvement with high sensitivity. The radiotracer accumulates in sites of increased osteoblastic activity and is therefore useful for confirming the diagnosis and performing follow-up (23).

Herpes Zoster Oticus

Herpes zoster oticus, also known as Ramsay Hunt syndrome, results from reactivation of latent varicella zoster virus infection in the geniculate ganglion of the facial nerve. It accounts for approximately 12% of all cases of peripheral nerve paralysis. It is rare in children, affects both sexes equally, and is usually unilateral. Clinically, herpes zoster oticus occurs with otalgia, auricular vesicles, and peripheral facial paralysis. In severe cases, involvement of the vestibulocochlear nerve may lead to sensorineural hearing loss and vestibular symptoms. The mainstay of treatment is a combination of antiviral and steroid medications.

MRI may show increased signal intensity on T2-weighted fluid-attenuated inversion-recovery images and paramagnetic contrast enhancement in one or more segments of the facial nerve, as compared with the unaffected side. Abnormal enhancement of the vestibular and cochlear nerves, structures of the membranous labyrinth, and even the pontine facial colliculus on the affected side also may occur (Fig 11) (26).

Relapsing Polychondritis

Relapsing polychondritis (RPC) is an immune-mediated systemic disease characterized by recurrent inflammatory episodes in cartilaginous and proteoglycan-rich tissues, including the elastic and hyaline cartilage of the ear, nose, tracheobronchial tree, and many other sites. The recurrent inflammation leads to anatomic deformation and dysfunction of the affected structures (Fig 12).

In more than 80% of patients, RPC manifests clinically as bilateral (or less commonly unilateral) auricular chondritis and polyarthritides, although many other organs potentially can be

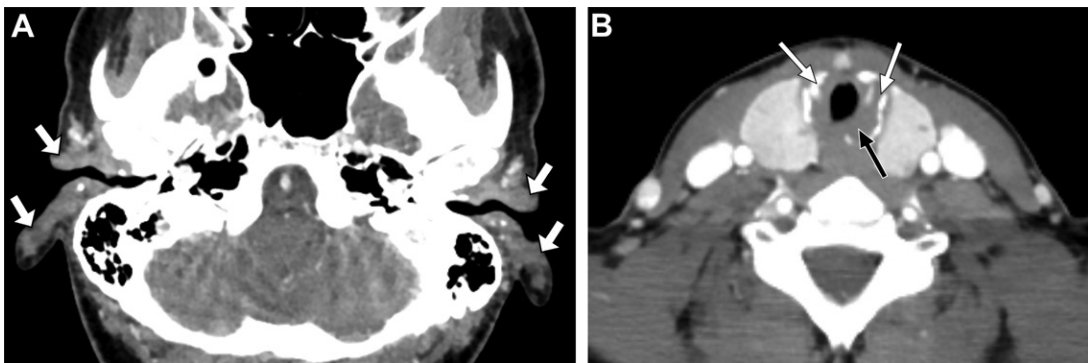


Figure 12. Relapsing polychondritis. Axial contrast-enhanced soft-tissue–window CT images at the levels of the temporal bone (A) and subglottic larynx (B) show diffuse thickening and enhancement of the auricle (arrows in A), a process that typically spares the ear lobe, and abnormal subglottic tissue thickening (black arrow in B), which is causing stenosis of the airway and fragmentation of the cricoid cartilage (white arrows in B).

involved (27). Acute painful inflammatory crises are followed by spontaneous remission of variable duration. In 30% of all adult patients with RPC, an association with other autoimmune disorders is found, with rheumatoid arthritis being the most common. The incidence of RPC peaks in the 5th decade of life; however, it has been described in young children and very elderly individuals and can affect all ethnic groups. A significant cause of mortality in patients with RPC is tracheobronchomalacia, as well as scarring with irreversible expiratory collapse of the tracheobronchial tree.

The diagnosis of RPC is made clinically, although laboratory tests and biopsy can be helpful. Although imaging is not routinely performed, CT images can show diffuse soft-tissue thickening in the cartilaginous portions of the EE, sparing the ear lobe (no cartilage component), without compromising the bony segments (Fig 12) (28).

Medial Canal Fibrosis

Medial canal fibrosis, or inflammatory acquired atresia of the EAC, is a benign acquired condition characterized by fibrous tissue formation in the medial part of the EAC after chronic otitis, surgery, radiation therapy, or trauma. It is bilateral in approximately 50% of cases.

Affected patients have conductive hearing loss, otorrhea, and/or a history of chronic otitis. Typical imaging findings include a crescent-shaped soft-tissue plug within the EAC, abutting the tympanic membrane. The bony walls of the EAC are preserved, and no erosion is seen (Fig 13) (29). The middle ear is normal. The differential diagnosis includes keratosis obturans (KO), EAC cholesteatoma, debris or cerumen impaction, and epithelial tumors.

Imaging does not always have capability for distinguishing medial canal fibrosis from KO,

which sometimes shows subtle EAC widening. The fact that EAC cholesteatoma shows permeative bony changes, which are not seen with medial canal fibrosis, also assists in differential diagnosis. Surgery is the treatment of choice, and topical antibiotics and steroids may help in the early stages of this disease.

EAC Cholesteatoma

A cholesteatoma is a lesion containing defoliating keratin lined by keratinizing stratified squamous epithelium with associated periostitis and bone erosion (30). Cholesteatomas may be acquired (in approximately 98% of cases) or congenital. Although they are found almost exclusively in the middle ear and mastoid air cells, in rare cases they occur in the EAC.

Patients with EAC cholesteatoma typically have otorrhea and chronic dull pain owing to local invasion of squamous tissue into the bony portion of the EAC (31). Most cases are idiopathic, with a predisposition to occur in the inferior medial aspect of the EAC. Secondary EAC cholesteatoma can occur in any area other than the inferior medial wall. Common predisposing factors are radiation therapy, surgery, and trauma to the canal. Preexisting EAC stenosis or obstruction also has been reported to cause EAC cholesteatoma. The clinical differential diagnosis includes neoplasms and inflammatory or infectious conditions such as KO, postinflammatory medial canal fibrosis, and necrotizing otitis externa (32).

EAC cholesteatoma affects older age groups and is usually unilateral. On CT images, the typical finding is a hypoattenuating mass with associated bony erosion and intralesion bone fragments. MR images show diffusion restriction in the soft-tissue mass, confirming the diagnosis (Fig 14) (33). Deep extension into the middle ear, mastoid air cells, facial nerve canal, or tegmen tympani can occur and must be reported

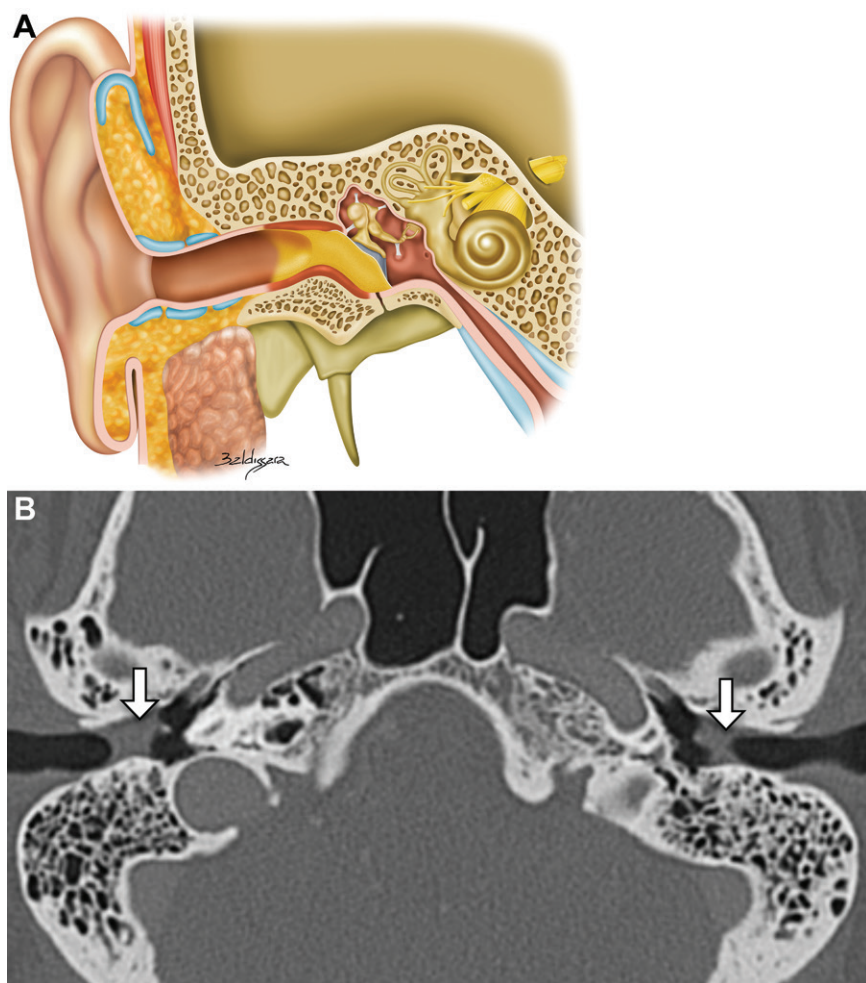


Figure 13. Medial canal fibrosis. Drawing (A) and axial bone-window CT image (B) show soft-tissue-attenuation material abutting the tympanic membrane, with a crescent-shaped lateral surface filling the medial bony portion of the EAC bilaterally (arrows in B). Note the lack of bony erosion or widening of the bony canal. Bilateral involvement is seen in approximately 50% of cases.

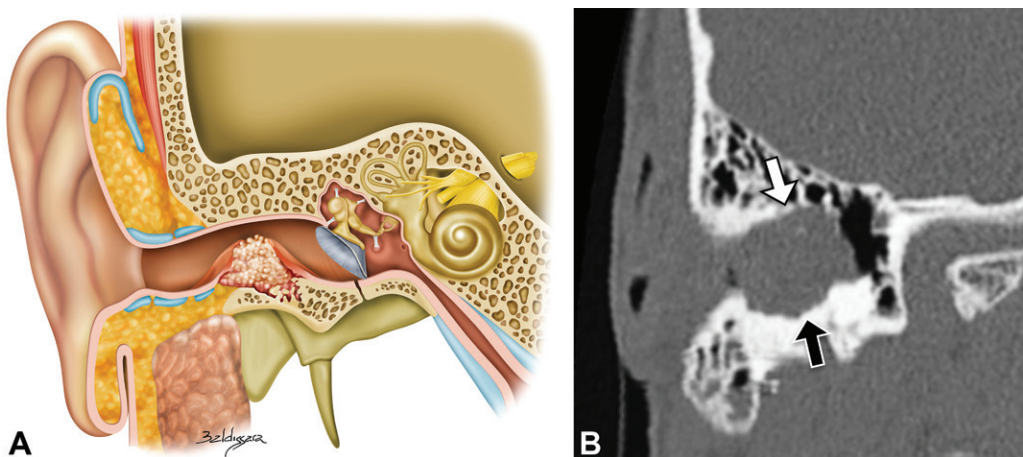


Figure 14. EAC cholesteatoma. Drawing (A) and coronal bone-window CT image (B) show a soft-tissue-attenuation mass occupying the bony portion of the EAC on the right (white arrow in B). Note the bone erosion in the inferior wall of the canal (black arrow in B), which is a characteristic feature of cholesteatoma. This finding is particularly useful for distinguishing cholesteatoma from other lesions such as KO and medial canal fibrosis, neither of which causes bone erosion.

Table 1: Diagnostic Features That Distinguish KO from EAC Cholesteatoma

Feature	KO	EAC Cholesteatoma
Age	Younger	Elderly
Pain	Acute	Chronic
Lateralization	Bilateral	Unilateral
Bone involvement	Circumferential remodeling	Focal erosion
Mental skin	Normal	Focal ulceration

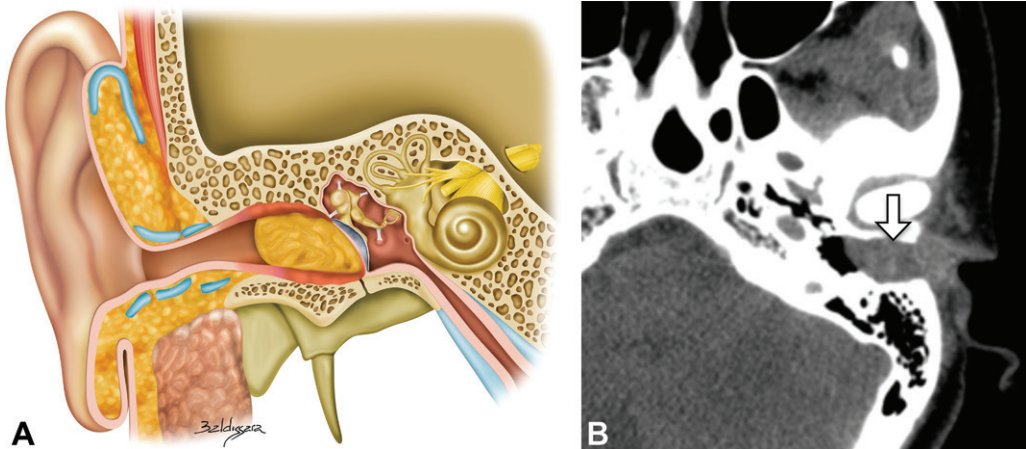


Figure 15. Keratosis obturans. Drawing (A) and axial soft-tissue–window CT image (B) show a soft-tissue–atenuation mass (arrow in B) occupying the EAC, with local mass effect and bulging of the tympanic membrane. No bone erosion is seen. There is slight focal expansion of the EAC at the level of the lesion.

whenever it is identified, as it usually influences surgical management (34).

Keratosis Obturans

KO is believed to be caused by sympathetic reflex stimulation of ceruminous glands within the EAC, leading to hyperemia and epidermal plugging. It results in accumulation of exfoliated keratin debris, without an enclosing sac of stratified squamous epithelium, within the EAC (5). KO was once believed to represent the same disease process as cholesteatoma but is now recognized as a separate entity (Table 1) (35). It manifests clinically as otalgia and conductive hearing loss due to keratin plugging and inflammation of the ear canal (36). Unlike cholesteatoma, KO occurs in younger patients and is often bilateral. Associations with bronchiectasis and sinusitis have been described.

CT images show a soft-tissue plug in the EAC with associated canal expansion due to remodeling, but no focal bone erosion or bone flecks within the mass, as seen with cholesteatoma (Fig 15) (Table 1). In contrast, MRI may show overlapping signal intensity features, since both KO and EAC cholesteatoma involve accumulation of desquamated keratin as the substrate. KO can nearly always be managed conservatively with use of regular aural toilet.

Benign Neoplasms

Exostosis and Osteoma

Exostosis of the EAC represents reactive osseous thickening of the EAC and is believed to be secondary to repetitive exposure to cold water and wind (Fig 16). The lesions are typically bilateral and multiple broad-based bone elevations that affect the tympanic bone (“surfer’s ear”) (3,35).

Exostoses differ from osteomas, which are regarded as true benign neoplasms and are usually unilateral, solitary, pedunculated, and located laterally within the EAC. Osteomas are associated with the tympanosquamous and tympanomastoid suture lines (3,35). CT images reveal a hyperattenuating pedunculated mass lateral to the isthmus within the EAC (Fig 17) (Table 2). Both exostoses and osteomas may lead to conductive hearing loss.

Benign Cutaneous Neoplasms

In addition to the usual benign cutaneous neoplasms elsewhere in the body, such as nevi and actinic keratoses, there is a small group of rare site-specific benign neoplasms recognized by the World Health Organization. These neoplasms originate from the ceruminous glands found in the cartilaginous segment of the EAC

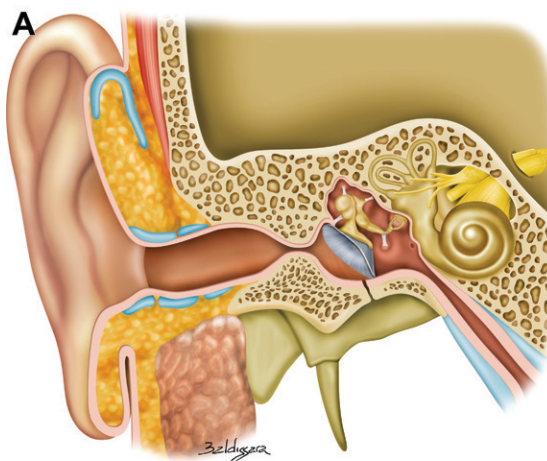


Figure 16. Exostosis. Drawing (A) and coronal bone-window CT image (B) show bone growth and thickening of the EAC bilaterally and symmetrically (arrows in B). Note the flat aspect of the lesions. Exostosis is frequently referred to as "surfer's ear" because of its association with cold water and wind exposure.

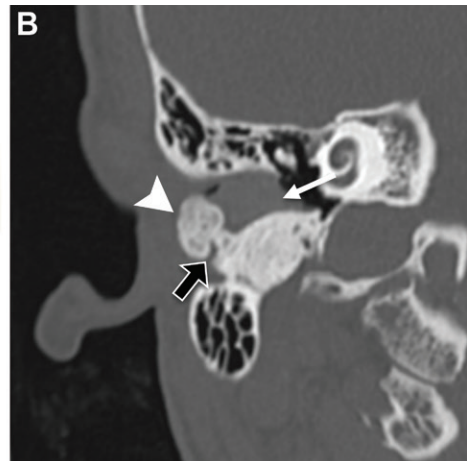
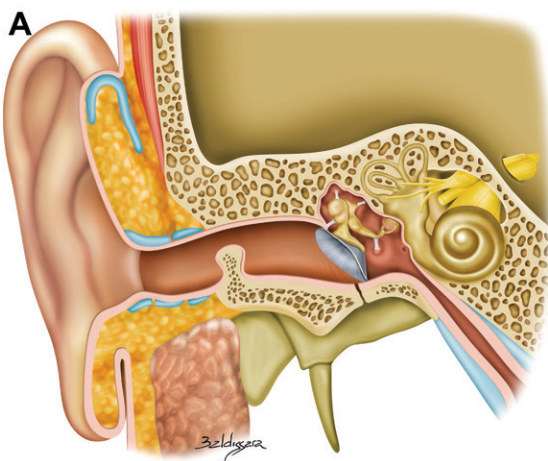


Figure 17. Osteoma. Drawing (A) and coronal bone-window CT image (B) show an expansile bony lesion of the right EAC (arrowhead in B) at the junction between the bony and cartilaginous portions of the canal, with a well-defined pedicle at the base (black arrow in B). The soft-tissue material filling the medial portion of the EAC (white arrow in B) represents cerumen buildup secondary to the mass effect of the lesion.

and include ceruminous adenoma, ceruminous pleomorphic adenoma, and syringocystadenoma papilliferum. These lesions are rare and occur as nonulcerated skin-covered masses (37).

Low-Flow Venous Malformations

Unlike infantile hemangioma, which is a typical true vascular neoplasm of newborns and infants, venous vascular malformations are not true neo-

plasms. Rather, they are congenital endothelial malformations that result from errors in vascular morphogenesis (38,39). Venous vascular malformation is one of the two most common slow- or low-flow vascular malformations and includes the lesions that used to be called cavernous hemangiomas (40–42). Involvement of the EE is rare but can cause conductive hearing loss. Venous vascular malformations can manifest

Table 2: Differentiating Diagnostic Features That Distinguish EAC Osteomas from EAC Exostoses

Feature	Osteoma	Exostosis
Pathophysiology	Benign neoplasm	Reactive osseous change
Lateralization	Unilateral	Bilateral
Manifestation	Pedunculated lesion	Broad-based bony overgrowth
Associations	Earwax, debris, or secondary cholesteatoma	None
Localization	Lateral in the EAC	Medial in the EAC

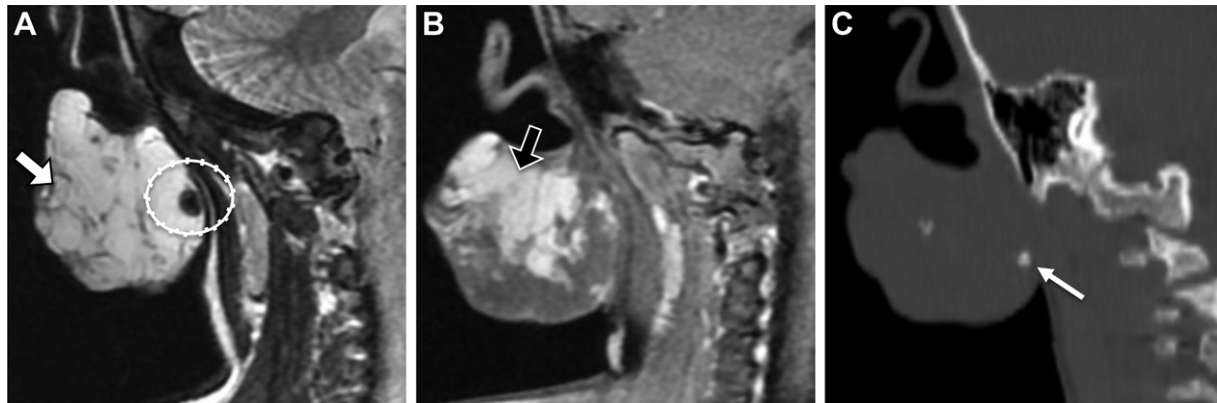


Figure 18. Low-flow venous malformation. (A, B) Coronal T2-weighted (A) and contrast-enhanced T1-weighted fat-suppressed (B) MR images show a large lobulated mass arising from the ear lobule. Note the thin septa (arrow in A) in the lesion and the typical early centripetal pattern of enhancement (arrow in B), with complete contrast material filling on images obtained later. (C) Coronal bone-window CT image shows phleboliths (arrow), which account for the hypointense foci seen in A (dotted circle).

radiologically as lobular or tubular masses with thrombi or phleboliths, the latter appearing as small round calcifications in the mass at CT.

Venous vascular malformations are hyperintense on T2-weighted MR images. Contrast enhancement is typical. Large lesions may have a progressive centripetal pattern of enhancement at CT or MRI when they are imaged early and late (after contrast material injection) (Fig 18). The Valsalva maneuver may cause enlargement of the mass by way of engorgement of the blood vessels (40–42).

Malignant Neoplasms

Malignancies of the EE can be primary, originating from the auricle and EAC, or secondary, due to direct tumor spread from an adjacent site (periauricular skin, parotid gland, or regional lymph nodes) (43,44).

Basal cell carcinoma is the most common malignant skin neoplasm, followed by squamous cell carcinoma and melanoma. Other rare malignant cutaneous neoplasms include lymphoma and Kaposi sarcoma (Fig 19). Cumulative sun exposure is the main risk factor for skin cancer.

Primary malignant neoplasm of the EAC is less common than its secondary involvement. Squamous cell carcinoma accounts for most cases, with long-standing chronic inflammation

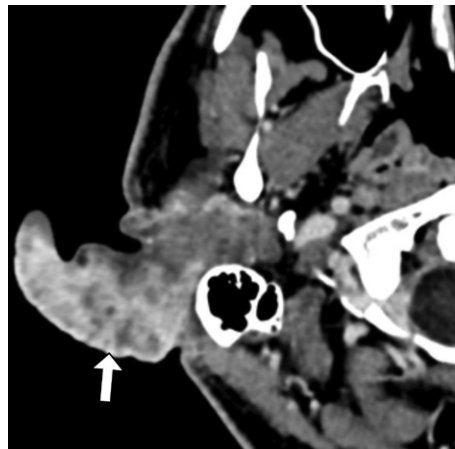


Figure 19. Biopsy-proven Kaposi sarcoma in a patient with HIV infection. Axial soft-tissue-window CT image shows a large, infiltrative, enhancing soft-tissue lesion (arrow) arising from the right auricle. Chest CT (not shown) showed multiple bilateral lung parenchymal consolidations with a flame-shaped appearance.

and prior radiation therapy as risk factors. Basal cell carcinoma, adenoid cystic carcinoma, and ceruminous adenocarcinoma are less common primary EAC malignancies (43,45).

Primary malignant tumors of the EAC tend to be misdiagnosed because they share symptoms

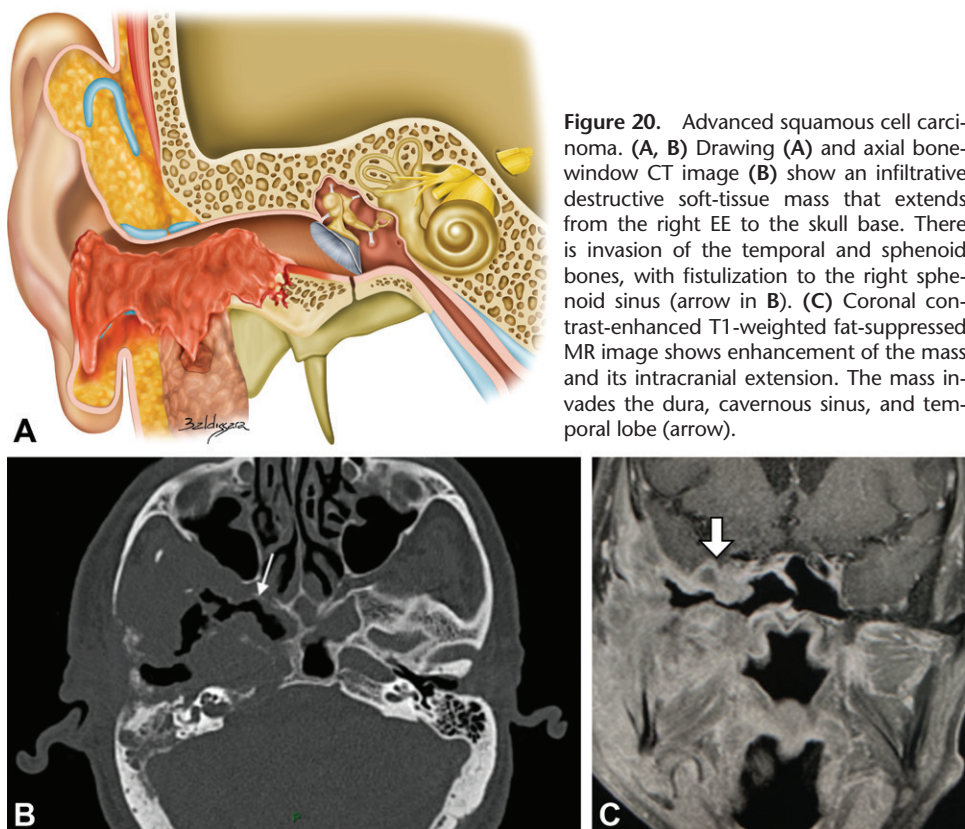


Figure 20. Advanced squamous cell carcinoma. (A, B) Drawing (A) and axial bone-window CT image (B) show an infiltrative destructive soft-tissue mass that extends from the right EE to the skull base. There is invasion of the temporal and sphenoid bones, with fistulization to the right sphenoid sinus (arrow in B). (C) Coronal contrast-enhanced T1-weighted fat-suppressed MR image shows enhancement of the mass and its intracranial extension. The mass invades the dura, cavernous sinus, and temporal lobe (arrow).

(otorrhea, otalgia, and hearing loss) with common conditions such as chronic suppurative otitis media and cholesteatoma (29,45).

Imaging plays an important role in assessment of malignant EE lesions, with the exception of those lesions clinically limited to the pinna and with low risk of nodal or distant metastasis. In the setting of primary or secondary malignant involvement of the EAC, CT is useful for identifying temporal bone involvement, showing osseous changes that range from slight to widespread destruction (Fig 20). Although erosion of the bony portion of the auditory canal is often the first sign of local tumor spread, care must be taken with regard to the anteroinferior wall, which may harbor an osseous pseudodeficit (focal thinning in 35% of healthy individuals, foramen of Huschke in <10% of healthy individuals) (46–48). On the other hand, the foramen of Huschke and fissures of Santorini are potential pathways for anterior spread of tumor and infectious processes (49).

MRI has some advantages over CT in the evaluation of tumors, including those confined to the ear and those spreading beyond the limits of the ear (Fig 20). Benign processes may be locally associated with a malignant lesion and thus lead to overestimation of the malignancy extension. While malignant neoplastic tissue shows moderate hyperintensity on T2-weighted images and

avid contrast enhancement, middle ear effusion and cholesteatoma are usually more hyperintense on these images and do not enhance (Fig 21). Cholesteatoma also shows higher diffusion restriction, helping distinguish it from an adjacent malignancy, which is usually less hypointense on apparent diffusion coefficient (ADC) maps (50). Indeed, water restriction in malignant neoplasms is variable on diffusion-weighted images and depends on the histologic tumor type.

MRI also enables better evaluation of tumor extension to the TMJ and parotid gland, as well as to the soft tissues around the ear, by depicting replacement of the T1-hyperintense fatty tissues with intermediate T1 signal intensity tumor, which also shows diffusion restriction and contrast enhancement. Intracranial extension, ranging from mild dural thickening to direct cerebral invasion, is well seen on coronal contrast-enhanced T1-weighted fat-suppressed MR images. Perineural tumor spread along cranial nerves VII and VIII also is best seen on contrast-enhanced T1-weighted fat-suppressed MR images (45,50).

The EE represents a watershed zone of lymphatic drainage; therefore, tumor spread to the anterior and posterior lymph nodes (parotid, periparotid, and perimastoid) as well as inferiorly to lymph node levels II and III can occur. As the most important prognostic predictor in patients with squamous cell carcinoma of the EE,

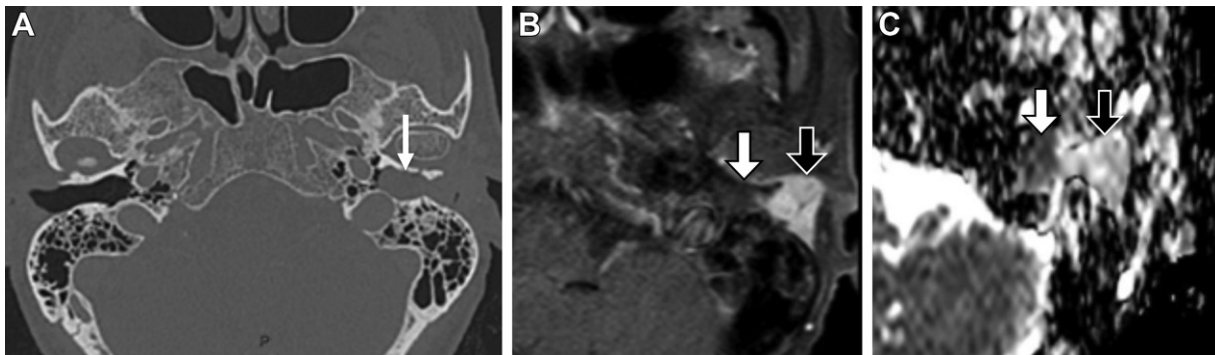


Figure 21. Adenoid cystic carcinoma. (A) Axial bone-window CT image shows a soft-tissue mass (arrow) abutting the tympanic membrane, with smooth widening of the EAC. (B, C) Corresponding axial contrast-enhanced T1-weighted fat-suppressed MR image (B) and apparent diffusion coefficient (ADC) map (C) show two distinct, readily identifiable components: The enhancing lateral component with high ADC (black arrow) corresponds to a biopsy-proven adenoid cystic carcinoma. The medial component, with restricted diffusion (low ADC) and lack of contrast enhancement (white arrow), represents a secondary cholesteatoma related to obstruction and impaired epithelial desquamation migration.

nodal involvement must be carefully inspected at clinical examination, and in cases of suspicion, contrast-enhanced CT should be the first-line diagnostic modality (50). Although locally aggressive, basal cell carcinoma is associated with extremely low rates of regional and distant metastasis (37). Lung metastasis is especially common with adenoid cystic carcinomas but rare with other EE neoplasms (45).

Osteoradionecrosis of the EAC

Radiation therapy is widely used as a primary or adjunctive therapy for head and neck malignancies (51). When the radiation field includes the temporal bone, osteoradionecrosis may develop as an uncommon but important late complication. The bony portion of the EAC is most affected, possibly because of its thin skin protection and unfavorable blood supply. There is usually a latent period, ranging from 1 to many years after completion of radiation treatment, before the onset of osteoradionecrosis, with trauma and infection being well-known triggers (52).

At otoscopy, an area of necrotic bone exposed through necrotic ulcerated skin is seen. Symptoms include pain, purulent or bloody otorrhea, and trismus if there is TMJ involvement (51). CT shows skin and bone erosions, bone sequestration and fragmentation, contrast enhancement, air within the soft tissues, and fluid within the mastoid air cells (Fig 22). Treatment is conservative or surgical (débridement) and can include hyperbaric oxygen therapy to enhance healing and provide symptom relief (53).

Miscellaneous Conditions

Foreign Body

Foreign bodies in the nose or ear are common causes of emergency department visits (54),

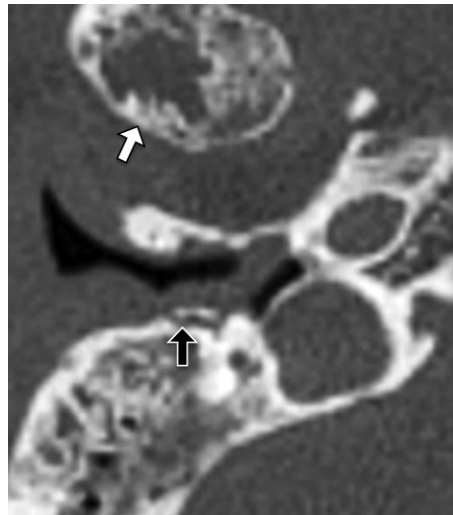


Figure 22. Osteoradionecrosis of the EAC in a patient with previous parotid adenocarcinoma, which was treated with surgical resection followed by radiation therapy 9 years previously. Axial bone-window CT image shows osteoradionecrosis (white arrow) of the mandibular head. Note the bone sequestration and fragmentation of the EAC (black arrow).

especially during childhood (Fig 23). All types of materials can be implicated and include paper, fabric, cotton wool or buds, rubber (eg, erasers), glass, beads, and live insects (55). The most appropriate imaging study for evaluation must be chosen on the basis of the suspected material. Dense materials such as metal, glass, and stone are clearly depicted on radiographs. CT is considered the reference standard for foreign-body imaging, allowing precise anatomic localization of hyperattenuating or hypotattenuating materials, including

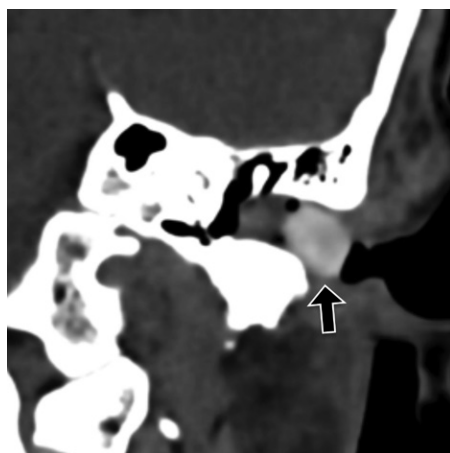


Figure 23. Foreign body. Coronal soft-tissue–window CT image shows a hyperattenuating foreign body (a bean seed) (arrow) obliterating the EAC, leading to accumulation of cerumen proximally within the canal.

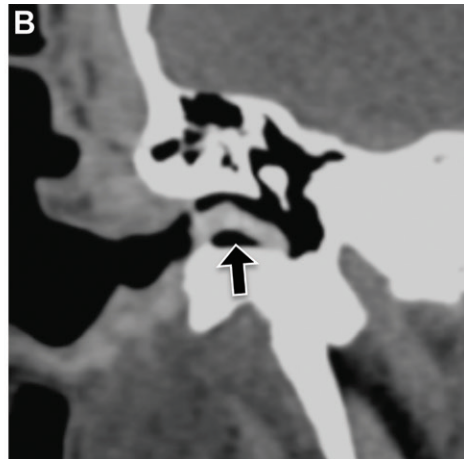
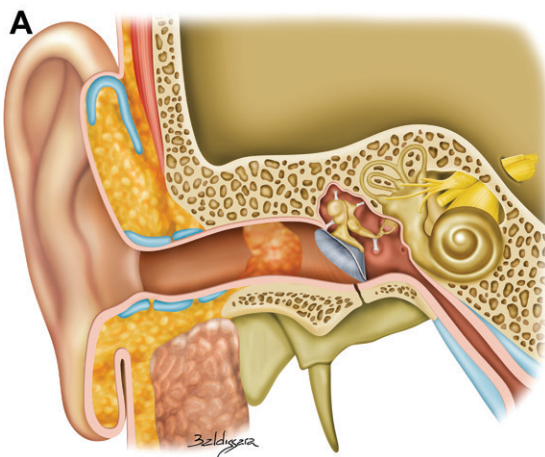


Figure 24. Cerumen. Drawing (A) and coronal soft-tissue–window CT image (B) show a soft-tissue lesion (arrow in B) filling the EAC, with a rim of air surrounding the cerumen. Note the lack of erosion or remodeling of the bony walls of the EAC. The attenuation should always be checked on soft-tissue–window CT images, as desiccated cerumen will have high attenuation.

wood and plastic (56). If not managed correctly, foreign bodies may lead to a series of complications, such as granuloma formation, laceration, tympanic membrane perforation, hearing loss, and canal edema (55).

Cerumen

Cerumen, or earwax, is a secretion produced by the ceruminous glands in the EAC. It has a protective role in the canal, including lubrication, waterproofing, and antibacterial properties (57). The presence of cerumen is physiologic, not pathologic, and is thus asymptomatic. However, excess buildup of cerumen may obstruct the EAC (cerumen impaction), blocking access to the middle and inner ear structures and causing symptoms that include hearing loss.

Imaging is not indicated in the absence of complications. When found incidentally on CT images, cerumen appears as hyperattenuating material when it is not hydrated (Fig 24), but it can have low attenuation at CT (1). Imaging

clues to help confirm the diagnosis of cerumen accumulation include nonadherence to the EAC wall, with a peripheral rim of air, and changes in appearance on consecutive imaging studies.

Cephalocele

Temporal bone cephalocele is a herniation of intracranial contents (meninges and/or brain) into the middle ear, mastoid air cells, petrous apex, or rarely the EAC (58–60). The cause of temporal bone cephalocele may be idiopathic, iatrogenic, or posttraumatic. Defects in the bony floor of the lateral skull base can lead to herniation of meningeal membranes or cerebral parenchyma, which manifests as a meningocele or meningoencephalocele, either of which is generically referred to as a cephalocele (61) or cerebrospinal fluid leakage. CT is the method of choice for identifying osseous defects, while MRI better depicts cephalocele contents. Cerebrospinal fluid has high signal intensity on T2-weighted MR images, while encephaloceles are isointense to brain parenchyma (Fig 25).

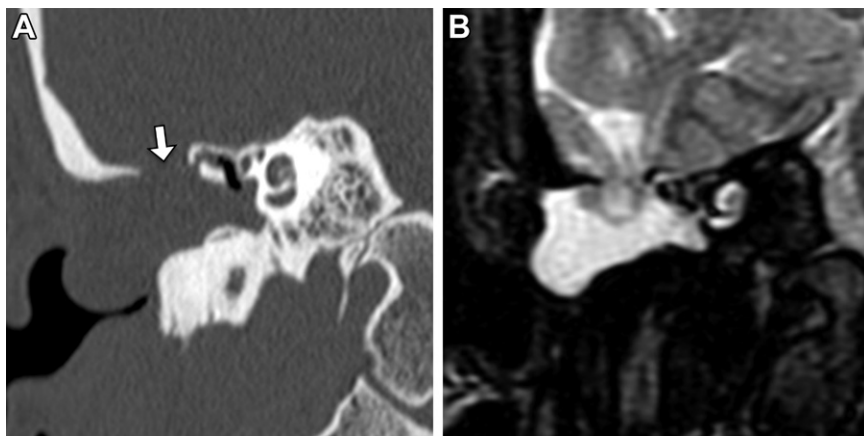


Figure 25. Cephalocele into the EAC. Coronal bone-window CT image (A) and coronal T2-weighted fat-suppressed MR image (B) show herniation of intracranial contents (cephalocele) through the roof of a bony defect (arrow in A) into the EAC. CT is the method of choice for evaluating the bony defect.

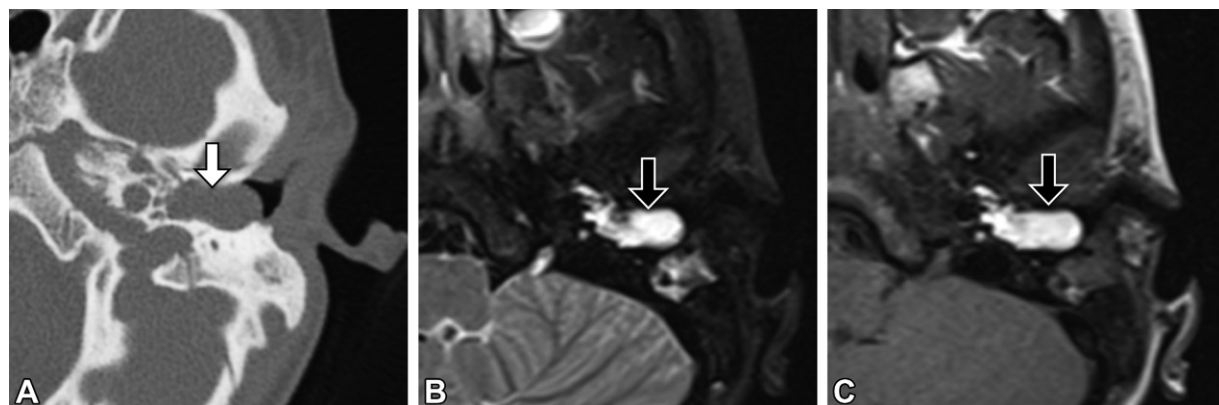


Figure 26. Cholesterol granuloma. (A) Axial bone-window CT image shows a soft-tissue-attenuation mass (arrow) occupying the osseous part of the left EAC. (B, C) Axial T2-weighted fat-suppressed (B) and T1-weighted (C) MR images show high signal intensity of the lesion (arrow), consistent with cholesterol granuloma, which was later surgically proven.

Cholesterol Granuloma

Cholesterol granulomas are benign granulomatous lesions caused by tissue reaction to a foreign body, namely cholesterol crystals (62,63). Some factors are believed to play an important role in development of cholesterol granulomas. These factors include drainage issues in certain structures, obstructed ventilation, and mucosal inflammation leading to hemorrhage and granuloma formation (62). The most common site of involvement is the petrous apex; involvement of the EAC is rare.

CT may reveal osseous erosions, and MRI shows T1 and T2 hyperintensity without internal contrast enhancement (Fig 26) (64). On T2-weighted images, a peripheral rim of low signal intensity resulting from hemosiderin deposition can be seen. Diffusion restriction is not common.

Conclusion

Pathologic conditions of the EE are usually diagnosed with clinical examination; imaging is often

not required. However, when needed, CT and MRI are the modalities of choice for evaluating the extent of the lesion and related complications. A flowchart to facilitate differential diagnosis of EE abnormalities is provided in Figure 27. Knowledge of the embryologic development and anatomy of the EE and familiarity with the most common and some less common associated conditions are essential for an accurate radiologic diagnosis.

Acknowledgment.—The authors thank Bruno Baldissara Moreira, Rio de Janeiro, Brazil, for his collaboration in preparing the medical illustrations.

References

1. Chatra PS. Lesions in the external auditory canal. Indian J Radiol Imaging 2011;21(4):274–278.
2. White RD, Ananthakrishnan G, McKean SA, Brunton JN, Hussain SS, Sudarshan TA. Masses and disease entities of the external auditory canal: radiological and clinical correlation. Clin Radiol 2012;67(2):172–181.
3. De Foer B, Kenis C, Vercruyse JP, et al. Imaging of temporal bone tumors. Neuroimaging Clin N Am 2009;19(3):339–366.
4. Juliano AF. Cross sectional imaging of the ear and temporal bone. Head Neck Pathol 2018;12(3):302–320.

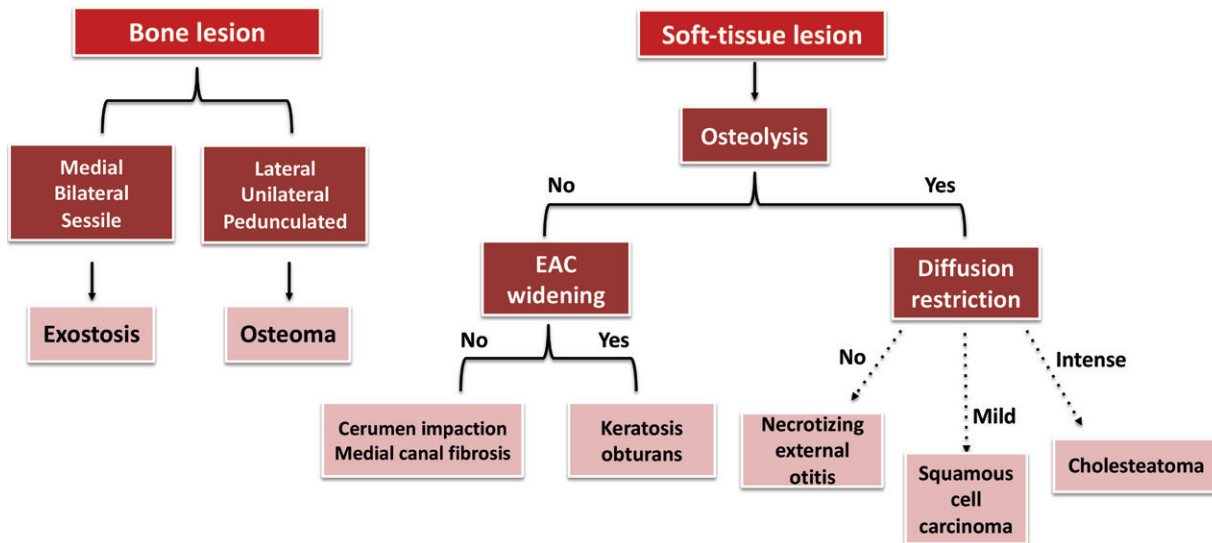


Figure 27. Flowchart outlines the differential diagnosis of EE lesions.

5. Juliano AF, Ginat DT, Moonis G. Imaging review of the temporal bone. I. Anatomy and inflammatory and neoplastic processes. *Radiology* 2013;269(1):17–33.
6. van der Meer WL, van Tilburg M, Mitea C, Postma AA. A persistent foramen of Huschke: a small road to misery in necrotizing external otitis. *AJNR Am J Neuroradiol* 2019;40(9):1552–1556.
7. Veugen CCAF, Dikkens FG, de Bakker BS. The developmental origin of the auricula revisited. *Laryngoscope* 2020;130(10):2467–2474.
8. Koch BL. Cystic malformations of the neck in children. *Pediatr Radiol* 2005;35(5):463–477.
9. Kösling S, Omenzetter M, Bartel-Friedrich S. Congenital malformations of the external and middle ear. *Eur J Radiol* 2009;69(2):269–279.
10. Benton C, Bellet PS. Imaging of congenital anomalies of the temporal bone. *Neuroimaging Clin N Am* 2000;10(1):35–53, vii–viii.
11. Mukerji SS, Parmar HA, Ibrahim M, Mukherji SK. Congenital malformations of the temporal bone. *Neuroimaging Clin N Am* 2011;21(3):603–619, viii.
12. Huang XY, Tay GS, Wansaicheong GK, Low WK. Preauricular sinus: clinical course and associations. *Arch Otolaryngol Head Neck Surg* 2007;133(1):65–68.
13. Cetin MA, Hatipoglu HG, Bilal N, Dere H, Dogan HT. A misdiagnosis: duplication of the external auditory canal. *Dentomaxillofac Radiol* 2009;38(2):116–120.
14. Stokroos RJ, Manni JJ. The double auditory meatus: a rare first branchial cleft anomaly—clinical presentation and treatment. *Am J Otol* 2000;21(6):837–841.
15. Zayas JO, Feliciano YZ, Hadley CR, Gomez AA, Vidal JA. Temporal bone trauma and the role of multidetector CT in the emergency department. *RadioGraphics* 2011;31(6):1741–1755.
16. Kurihara YY, Fujikawa A, Tachizawa N, Takaya M, Ikeda H, Starkey J. Temporal bone trauma: typical CT and MRI appearances and important points for evaluation. *RadioGraphics* 2020;40(4):1148–1162.
17. Dang D. Bilateral mandibular condylar fractures with associated external auditory canal fractures and otorrhagia. *Radiol Case Rep* 2016;2(1):24–29.
18. Wood CP, Hunt CH, Bergen DC, et al. Tympanic plate fractures in temporal bone trauma: prevalence and associated injuries. *AJNR Am J Neuroradiol* 2014;35(1):186–190.
19. Rosenfeld RM, Schwartz SR, Cannon CR, et al. Clinical practice guideline: acute otitis externa. *Otolaryngol Head Neck Surg* 2014;150(1 suppl):S1–S24.
20. Roland PS, Stroman DW. Microbiology of acute otitis externa. *Laryngoscope* 2002;112(7 pt 1):1166–1177.
21. Rubin Grandis J, Branstetter BF 4th, Yu VL. The changing face of malignant (necrotising) external otitis: clinical, radiological, and anatomic correlations. *Lancet Infect Dis* 2004;4(1):34–39.
22. Grandis JR, Curtin HD, Yu VL. Necrotizing (malignant) external otitis: prospective comparison of CT and MR imaging in diagnosis and follow-up. *Radiology* 1995;196(2):499–504.
23. Alvarez Jáñez F, Barriga LQ, Iñigo TR, Roldán Lora F. Diagnosis of skull base osteomyelitis. *RadioGraphics* 2021;41(1):156–174.
24. Kwon BJ, Han MH, Oh SH, Song JJ, Chang KH. MRI findings and spreading patterns of necrotizing external otitis: is a poor outcome predictable? *Clin Radiol* 2006;61(6):495–504.
25. Mani N, Sudhoff H, Rajagopal S, Moffat D, Axon PR. Cranial nerve involvement in malignant external otitis: implications for clinical outcome. *Laryngoscope* 2007;117(5):907–910.
26. Sartoretti-Schefer S, Kollas S, Valavanis A. Ramsay Hunt syndrome associated with brain stem enhancement. *AJNR Am J Neuroradiol* 1999;20(2):278–280.
27. Mathian A, Miyara M, Cohen-Aubert F, et al. Relapsing polychondritis: a 2016 update on clinical features, diagnostic tools, treatment and biological drug use. *Best Pract Res Clin Rheumatol* 2016;30(2):316–333.
28. Faix LE, Branstetter BF 4th. Uncommon CT findings in relapsing polychondritis. *AJNR Am J Neuroradiol* 2005;26(8):2134–2136.
29. Trojanowska A, Drop A, Trojanowski P, Rosinska-Bogusiewicz K, Klatka J, Bobek-Billewicz B. External and middle ear diseases: radiological diagnosis based on clinical signs and symptoms. *Insights Imaging* 2012;3(1):33–48.
30. Persaud RA, Hajioff D, Thevasagayam MS, Wareing MJ, Wright A. Keratosis obturans and external ear canal cholesteatoma: how and why we should distinguish between these conditions. *Clin Otolaryngol Allied Sci* 2004;29(6):577–581.
31. Owen HH, Rosborg J, Gaihede M. Cholesteatoma of the external ear canal: etiological factors, symptoms and clinical findings in a series of 48 cases. *BMC Ear Nose Throat Disord* 2006;6(1):16.
32. Heilbrun ME, Salzman KL, Glastonbury CM, Harnsberger HR, Kennedy RJ, Shelton C. External auditory canal cholesteatoma: clinical and imaging spectrum. *AJNR Am J Neuroradiol* 2003;24(4):751–756.
33. Baráth K, Huber AM, Stämpfli P, Varga Z, Kollas S. Neuroradiology of cholesteatomas. *AJNR Am J Neuroradiol* 2011;32(2):221–229.
34. Shin SH, Shim JH, Lee HK. Classification of external auditory canal cholesteatoma by computed tomography. *Clin Exp Otorhinolaryngol* 2010;3(1):24–26.
35. Touska P, Juliano AF. Temporal bone tumors: an imaging update. *Neuroimaging Clin N Am* 2019;29(1):145–172.

36. Shinnabe A, Hara M, Hasegawa M, et al. A comparison of patterns of disease extension in keratosis obturans and external auditory canal cholesteatoma. *Otol Neurotol* 2013;34(1):91–94.
37. Sand M, Sand D, Brors D, Altmeyer P, Mann B, Bechara FG. Cutaneous lesions of the external ear. *Head Face Med* 2008;4(1):2.
38. Brouillard P, Viikkula M. Vascular malformations: localized defects in vascular morphogenesis. *Clin Genet* 2003;63(5):340–351.
39. Fishman SJ, Mulliken JB. Hemangiomas and vascular malformations of infancy and childhood. *Pediatr Clin North Am* 1993;40(6):1177–1200.
40. Kollipara R, Odhav A, Rentas KE, Rivard DC, Lowe LH, Dinneen L. Vascular anomalies in pediatric patients: updated classification, imaging, and therapy. *Radiol Clin North Am* 2013;51(4):659–672.
41. Navarro OM, Laffan EE, Ngan BY. Pediatric soft-tissue tumors and pseudo-tumors: MR imaging features with pathologic correlation. I. Imaging approach, pseudotumors, vascular lesions, and adipocytic tumors. *RadioGraphics* 2009;29(3):887–906.
42. Restrepo R. Multimodality imaging of vascular anomalies. *Pediatr Radiol* 2013;43(suppl 1):S141–S154.
43. Allanson BM, Low TH, Clark JR, Gupta R. Squamous cell carcinoma of the external auditory canal and temporal bone: an update. *Head Neck Pathol* 2018;12(3):407–418.
44. Lovin BD, Gidley PW. Squamous cell carcinoma of the temporal bone: a current review. *Laryngoscope Investig Otolaryngol* 2019;4(6):684–692.
45. Xia S, Yan S, Zhang M, et al. Radiological findings of malignant tumors of external auditory canal: a cross-sectional study between squamous cell carcinoma and adenocarcinoma. *Medicine (Baltimore)* 2015;94(35):e1452.
46. Hosokawa S, Mizuta K, Takahashi G, et al. Surgical approach for treatment of carcinoma of the anterior wall of the external auditory canal. *Otol Neurotol* 2012;33(3):450–454.
47. Lacout A, Marsot-Dupuch K, Smoker WR, Lasjaunias P. Foramen tympanicum, or foramen of Huschke: pathologic cases and anatomic CT study. *AJNR Am J Neuroradiol* 2005;26(6):1317–1323.
48. Ong CK, Pua U, Chong VF. Imaging of carcinoma of the external auditory canal: a pictorial essay. *Cancer Imaging* 2008;8(1):191–198.
49. Gillespie MB, Francis HW, Chee N, Eisele DW. Squamous cell carcinoma of the temporal bone: a radiographic-pathologic correlation. *Arch Otolaryngol Head Neck Surg* 2001;127(7):803–807.
50. Wang Z, Zheng M, Xia S. The contribution of CT and MRI in staging, treatment planning and prognosis prediction of malignant tumors of external auditory canal. *Clin Imaging* 2016;40(6):1262–1268.
51. Sharon JD, Khwaja SS, Drescher A, Gay H, Chole RA. Osteoradionecrosis of the temporal bone: a case series. *Otol Neurotol* 2014;35(7):1207–1217.
52. Metselaar M, Dumans AG, van der Huls MP, Sterk W, Feenstra L. Osteoradionecrosis of tympanic bone: reconstruction of outer ear canal with pedicled skin flap, combined with hyperbaric oxygen therapy, in five patients. *J Laryngol Otol* 2009;123(10):1114–1119.
53. Ahmed S, Gupta N, Hamilton JD, Garden AS, Gidley PW, Ginsberg LE. CT findings in temporal bone osteoradionecrosis. *J Comput Assist Tomogr* 2014;38(5):662–666.
54. Mackle T, Conlon B. Foreign bodies of the nose and ears in children: should these be managed in the accident and emergency setting? *Int J Pediatr Otorhinolaryngol* 2006;70(3):425–428.
55. Schulze SL, Kerschner J, Beste D. Pediatric external auditory canal foreign bodies: a review of 698 cases. *Otolaryngol Head Neck Surg* 2002;127(1):73–78.
56. Voss JO, Maier C, Wüster J, et al. Imaging foreign bodies in head and neck trauma: a pictorial review. *Insights Imaging* 2021;12(1):20.
57. Prokop-Prigge KA, Thaler E, Wysocki CJ, Preti G. Identification of volatile organic compounds in human cerumen. *J Chromatogr B Analys Technol Biomed Life Sci* 2014;953:954:48–52.
58. Alijani B, Bagheri HR, Chabok SY, Behzadnia H, Dehghani S. Posttraumatic temporal bone meningocele presenting as a cystic mass in the external auditory canal. *J Craniofac Surg* 2016;27(5):e481–e484.
59. Kamerer DB, Caparosa RJ. Temporal bone encephalocele: diagnosis and treatment. *Laryngoscope* 1982;92(8 pt 1):878–882.
60. Vaezi A, Snyderman CH, Saleh HA, Carrau RL, Zanation A, Gardner P. Pseudomeningoceles of the sphenoid sinus masquerading as sinus pathology. *Laryngoscope* 2011;121(12):2507–2513.
61. Naidich TP, Altman NR, Braffman BH, McLone DG, Zimmerman RA. Cephaloceles and related malformations. *AJNR Am J Neuroradiol* 1992;13(2):655–690.
62. Kong JS, Kim MS, Lee KY. A case of a cholesterol granuloma occluding the external auditory canal in a 12-year-old girl. *Korean J Audiol* 2014;18(2):89–92.
63. Nager GT, Vanderveen TS. Cholesterol granuloma involving the temporal bone. *Ann Otol Rhinol Laryngol* 1976;85(2 pt 1):204–209.
64. Nikolaidis V, Malliari H, Psifidis D, Metaxas S. Cholesterol granuloma presenting as a mass obstructing the external ear canal. *BMC Ear Nose Throat Disord* 2010;10(1):4.